



HHS Public Access

Author manuscript

J Nutr Biochem. Author manuscript; available in PMC 2020 April 16.

Published in final edited form as:

J Nutr Biochem. 2018 December ; 62: 123–133. doi:10.1016/j.jnutbio.2018.09.003.

Flavin homeostasis in the mouse retina during aging and degeneration

Tirthankar Sinha¹, Mustafa Makia¹, Jianhai Du², Muna I. Naash^{1,*}, Muayyad R. AlUbaidi^{1,*}

¹Department of Biomedical Engineering, University of Houston, Houston, TX 77204

²Department of Ophthalmology and Department of Biochemistry, West Virginia University, Morgantown, WV 26506

Abstract

Involvement of flavin adenine dinucleotide (FAD) and flavin mononucleotide (FMN) in cellular homeostasis has been well established for tissues other than the retina. Here, we present an optimized method to effectively extract and quantify FAD and FMN from a single neural retina and its corresponding retinal pigment epithelium (RPE). Optimizations led to detection efficiency of 0.1 pmol for FAD and FMN while 0.01 pmol for riboflavin. Interestingly, levels of FAD and FMN in the RPE were found to be 1.7 and 12.5 folds higher than their levels in the retina, respectively. Both FAD and FMN levels in the RPE and retina gradually decline with age and preceded the age-dependent drop in the functional competence of the retina as measured by electroretinography. Further, quantifications of retinal levels of FAD and FMN in different mouse models of retinal degeneration revealed differential metabolic requirements of these two factors in relation to the rate and degree of photoreceptor degeneration. We also found 2 fold reductions in retinal levels of FAD and FMN in two mouse models of diabetic retinopathy. Altogether, our results suggest that retinal levels of FAD and FMN can be used as potential markers to determine state of health of the retina in general and more specifically the photoreceptors.

Keywords

retina; flavins; retinal degeneration; riboflavin; flavin adenine dinucleotide; flavin adenine mononucleotide

1. Introduction

Riboflavin (RF, aka vitamin B2) belongs to the class of water soluble vitamins and is essential for production of biological energy [1]. It is absorbed from diet by specific

*To whom correspondence should be addressed at: Department of Biomedical Engineering, University of Houston, 3517 Cullen Blvd., Houston, TX 77204, USA, mnaash@central.uh.edu and mlubaid@central.uh.edu., +1-713-743-1651 and +1-713-743-1649.

Conflict of Interest Statement

The authors declare no conflicts of interests.

Publisher's Disclaimer: This is a PDF file of an unedited manuscript that has been accepted for publication. As a service to our customers we are providing this early version of the manuscript. The manuscript will undergo copyediting, typesetting, and review of the resulting proof before it is published in its final citable form. Please note that during the production process errors may be discovered which could affect the content, and all legal disclaimers that apply to the journal pertain.

intestinal receptors and then transported to other tissue based on their energetic mandates [2, 3]. Depending upon cellular requirements, part of the internalized RF is then enzymatically converted to RF active phosphorylated derivatives, FAD (Flavin adenine dinucleotide) and FMN (Flavin mononucleotide) [4]. The rest of RF has a short half-life and is quickly cleared from the body [5].

Subsequently, FAD and FMN not only act as cofactors for various enzymes involved in oxidation-reduction (redox) reactions, they are utilized for deriving other essential cofactors involved in metabolism [6]. FAD and FMN are also essential for the function of other vitamins like pyridoxine and nicotinic acid [7]. The direct involvement of FAD and FMN as rate limiting factors in energy metabolism is well documented and it is well understood that there is a direct correlation between the rate of energy metabolism of a specific cell with the cellular levels of FAD and FMN [8].

Levels of FAD and FMN in different organs vary depending on the requirements of that organ. For example, compared to the blood, the retina retains high concentrations of FAD and FMN [9]. This is not surprising since retinal photoreceptors are among the most metabolically active cells in the body [10–13]. Although the correlation between reduced FAD and FMN levels and clinically relevant pathologies has been well documented [14–16], limited information is available about their retinal levels in physiological and pathological conditions [17, 18]. Moreover, these reports date back decades and given the advancement in separation technology, it is essential to develop an improved, more sensitive method for their detection and quantification.

The direct involvement of FAD and FMN as cofactors for essential metabolic pathways underlines the importance of their quantitation in aging and metabolic pathologies. It is well known that aging is associated with downregulation of oxidative phosphorylation and decline in mitochondrial energy metabolism [19–21]; both are linked to flavin levels. Furthermore, retinal metabolic pathologies are significantly affected in diabetic retinopathy, which may stem from the metabolic dysfunction of photoreceptors [22], which consume most of the oxygen that enters the retina [23]. This underscores the necessity to quantify the levels of FAD and FMN during the progression of diabetic retinopathy.

Herein, we have modified and optimized the previously reported micro-extraction of FAD and FMN using a single retina and its corresponding RPE [9] and significantly increased the sensitivity of HPLC detection. Furthermore, we report on the steady state levels of flavins in the mouse retina and retinal pigment epithelium (RPE), independently. We also determined the effect of physiological conditions such as fasting and aging on the steady state levels of retinal flavins. Finally, we selected well studied animal models of retinal degeneration and metabolic dysfunction to quantify flavins in the retina and the RPE. Our data indicate that changes in flavin levels may be a precursor for metabolic changes occurring before or during the degenerative process.

2. Materials and Methods

2.1 Chemicals and reagents

FAD and FMN standards (95% purity) and RF (98% purity) were purchased from Sigma-Aldrich, St. Louis, MO, USA. Acetonitrile (HPLC grade), trichloroacetic acid (TCA), phosphoric acid and 0.45µmX4mm nylon syringe filter (F25041) were purchased from Fisher Scientific (Hanover Park, IL). Ultrapure water was obtained from a Milli-Q Integral 3 Water Purification System (Billerica, MA).

2.2 Animals and tissue collection

Animal experiments were approved by the University of Houston Institutional Animal Care and Use Committee (IACUC) and adhered to recommendations in NIH Guide for the Care and Use of Laboratory Animals and the Association for Research in Vision and Ophthalmology. All mice were on C5BL/6 background (C57BL/6–129SV strain for the ones used for HPLC and C57BL/6 for those used for the LC-MS) and were genotyped for and found to be negative for both the rd8 allele [24] and the RPE65 Leu450Met variant [25, 26]. Animals were reared under cyclic light conditions (12 hours L/D, ~30 lux). The euthanasia of mice was by CO₂ asphyxiation followed by decapitation. Retina and/or PECS (retinal pigment epithelium, choroid and sclera) were harvested and used as indicated below. For isolation of retina, a pair of fine forceps was used to dilate the eye and using a fine surgical blade, a fine cut was made across the top of the cornea. Subsequently, the anterior segments of the eye (cornea, lens and iris) were removed out. Then using the fine forceps, the entire retina with all its layers were teased out and snap frozen. From the rest of the eyecup, the PECS complex was dissected, taking care that no optic nerve or blood is associated. This PECS complex has been referred to as RPE elsewhere in the text, unless otherwise mentioned.

2.3 Micro-extraction of flavins

Tissues were extracted and either used fresh or snap frozen and stored at –80°C until use. All subsequent steps were carried out in the dark and on ice unless indicated. Tissues were homogenized using a handheld motor and pestle (VWR, Radnor, PA, USA) in 100µl of 1X PBS (pH 6.8 unless otherwise indicated) and a 30µl aliquot was saved for protein assay. Remainder was centrifuged at 1,000Xg for 10 minutes at 4°C and supernatant was separated and incubated at 37°C in 10% TCA (optimized by using 5%, 10% and 25%) for 15 minutes to precipitate proteins.

Resultant was centrifuged at 10,000Xg for 10 minutes at 4°C; supernatant was carefully collected, filtered through 0.45µm filter and used for HPLC analysis. To minimize the effect of freeze thaw, injection of samples into the HPLC system was done right after extraction for all the samples, without freezing them.

It was previously shown by Bessey *et al* [27] that with 10% TCA there is no acid hydrolysis of FAD and FMN as long as samples are kept on ice. Acid hydrolysis only happens if samples with 10% TCA were kept in 15 °C (40 mins) or even more so when kept at 37°C (20 mins).

2.4 HPLC Chromatography

The mobile phase was optimized using varying concentrations of phosphate buffer (10, 50 and 100 mM) and at pH (3.1 and 5.5). In order to distinctly generate well defined peaks for FAD, FMN and RF, the flow rate and percent of acetonitrile were varied using a gradient method as described in section 3.1. No TCA was used in as an HPLC solvent modifier. The HPLC setup was composed of Waters binary HPLC pump (1525), Waters auto-sampler (2707), Waters multi wavelength fluorescence detector (2475) and a Waters X-Bridge C18 3.5 μ m column with dimensions of 4.6X250mm (Waters, Milford, MA, USA).

2.5 HPLC quantification of flavins

For retinal flavin identification, extracts from the respective tissues were separately spiked with each of the standards as well as with all three flavins. Subsequently, different concentrations of the three standards were mixed together and were used to generate a standard curve for each of the compounds based on the area under the curve as calculated by the Breeze 2 software (Waters, Milford, MA, USA). Different concentrations of standards for each of FAD, FMN and RF were injected and quantified for linearity. A processing method was generated using identified retention times and standard curve plotted for each component, integrated to auto-identify the peaks and auto-calculate the concentration of the respective compounds. The concentration values of FAD and FMN extracted from the specific tissues were normalized to total tissue protein. Protein concentrations were determined by Bradford assay (BioRad, Hercules, California), with Bovine serum albumin (BSA) used as the protein standard.

For the diabetic models, the flavin values were represented as per retina instead of per mg protein since protein levels would vary significantly based on the pathology of degeneration [28–30].

2.6 Flavin quantification by LC MS/MS

Samples were prepared and analyzed as described before with minor modification [31]. Briefly, the retinas and RPE were independently homogenized in cold 80% methanol (methanol:water (80:20 V/V)) using a microtube homogenizer and stored on dry ice for 30 min. After centrifugation at 15,000 RPM for 10 min, the supernatant was transferred and dried using the FreeZone 4.5 L freeze dryer (Labconco, Kansas City, MO). Samples were reconstituted with 100 μ l of mobile phase (a mixture of A:B (below) at 40:60 in V/V) for LC MS/MS. The extracts were analyzed by a Shimadzu LC Nexera X2 UHPLC coupled with a QTRAP 5500 LC MS/MS (AB Sciex). An ACQUITY UPLC UPLC BEH Amide analytic column (2.1 X 50 mm, 1.7 μ m, Waters) was used for chromatographic separation. The mobile phase was (A) water with 10 mM ammonium acetate (pH 8.9) and (B) acetonitrile/water (95/5) with 10 mM ammonium acetate (pH 8.2). All solvents were LC-MS Optima grade from Fisher Scientific. The total run time was 11 mins with a flow rate of 0.5 mL/min with an injection volume of 5 μ l. The gradient elution is 95–61% B in 6 min, 61–44% B at 8 min, 61–27% B at 8.2 min, and 27–95% B at 9 min. The column was equilibrated with 95% B at the end of each run. The source and collision gas was N₂. The ion source conditions in positive and negative mode were: curtain gas (CUR) = 25 psi, collision gas (CAD) = high, ion spray voltage (IS) = 3800/–3800 volts, temperature (TEM) = 500°C, ion source gas 1

(GS1) = 50 psi, and ion source gas 2 (GS2) = 40 psi. Each metabolite was tuned with standards for optimal transitions. ¹³C-nicotinic acid (Toronto Research Chemicals, Toronto, Ontario) was used as the internal standard. The extracted MRM peaks were integrated using MultiQuant 3.0.2 software (Framingham, MA).

2.7 Electroretinography

Full field electroretinograms (ERG) were recorded as previously described [32]. Prior to ERG, mice were dark adapted overnight. Mice were anesthetized by intramuscular injection of 85 mg/kg ketamine and 14 mg/kg xylazine and eyes were dilated using 1% cyclogyl (Pharmaceutical Systems Inc., Tulsa, OK). ERG light-evoked responses were recorded with a UTAS system (LKC, Gaithersburg, MD, USA). The ERG stimulus was recorded with a platinum wire loop electrode in contact with the cornea through a methyl cellulose layer (Pharmaceutical Systems Inc.). Scotopic ERGs (rod photoreceptor function) were recorded with a strobe flash stimulus of 157 cd-s/m². Photopic (cone photoreceptor responses) ERG was recorded from 25 averaged flashes at 157 cds/m² for white light, 12.5 cd-s/m² for green light (530 nm) and 0.79 cd-s/m² for UV light (365 nm), following a 5 min light adaptation with background light at an intensity of 29.03 cd/m².

2.8 Statistical analysis

Data is presented as mean ± S.E.M. unless otherwise mentioned and the number of samples used for each experiment is mentioned as n in the respective figure legends. All the statistical analyses were performed using the GraphPad Prism 7.00 (GraphPad Software, La Jolla, CA, USA) with P values reported for each measurement.

3. Results

3.1. Tissue extraction and HPLC quantification of steady state levels of flavins.

We first adapted the tissue extraction and HPLC quantification procedures reported by Batey [9] with the modifications listed below. In that study, samples were heated during the extraction [9] but we chose to perform our extractions on ice, unless stated otherwise. The rationale provided by the authors for heating was to release the loosely bound flavins from the respective flavoproteins. However, the authors also report that there is loss in FAD and FMN upon heating. This is similar to other recent papers reporting thermal degradation of both FAD and FMN [33], even though riboflavin is known to be highly thermostable [34]. Thus performing all the extraction steps on ice was critical to prevent any hydrolysis of FAD to FMN and further into riboflavin and enabling us to measure the stable physiological levels of both FAD and FMN. Since precipitation by 10% TCA alone is able to effectively dissociate flavins from flavoproteins [35–37] without affecting the stability of FAD and FMN, we chose to perform the 10% TCA precipitation without heating the samples. Another difference is that our flavin extractions were in phosphate buffer saline (pH=5.5), which has been frequently used for flavin quantitation from various sources, without affecting the stability of FAD and FMN [38]. To develop an HPLC gradient method for flavins, the standards were first used to generate a six point concentration curve using linear regression analysis (as described in the Method Section). Whether all three flavins were pooled together or used separately, no change in individual retention time was observed. This

indicates that the chemical composition of each flavin does not interfere with the elution time of the others (Fig. 1). In Batey's study [9], isocratic method was used to separate flavins by HPLC but we found it leads to overlapping peaks of FAD and FMN. After further optimization, we found complete separation of the three flavins by using a gradient method, mixing solution A (50 mM phosphate buffer, pH=3) and solution B (100% acetonitrile) at a flow rate of 0.8 ml/minute (Fig. 1D). Table 1 shows the adopted optimized method with the shortest run time. The observed retention times for FAD, FMN, and RF are 16.9, 18.1, and 19.2 min, respectively. The initial 6.25 min of the run with 95% solution A and 5% solution B was to equilibrate the column and to enhance the retention efficiency of flavins. Sequential elution of flavins happens with gradual increase in solution B and simultaneous reduction in solution A. This process is completed at 19.2 min (Fig. 1). The 3–4 min portion of the run profile of the column at 50% of solution A and 50% of solution B corresponds to column clean-up and the elution of any un-eluted components. The column is then re-calibrated to the initial condition for ~6 min with 95% solution A and 5% solution B before testing the next sample.

All flavins gave good correlation coefficient (r) values as shown in Table 2, which also includes regression parameters such as slopes and intercepts. The limit of quantification (LoQ) for all flavins is substantially lower than the 2 pmol for all flavins detected in prior studies using an isocratic method [9]. Our LoQ values were 0.1 pmol for FAD and FMN while 0.01 pmol for RF.

The accuracy of our extraction method was confirmed by performing recovery analyses of independent retina and RPE samples spiked with equal amounts of FAD, FMN and RF. As shown in Table 3, the recovery from the retina was 98.6 ± 1.3 for FAD, 99.2 ± 2.7 for FMN and 96.2 ± 6.1 for RF and from the RPE was 97.3 ± 4.6 for FAD, 97.1 ± 3.3 for FMN and 95.1 ± 1.1 for RF. This optimized extraction procedure of flavins from the retina and RPE was used for the remaining analyses performed in this study. Spiking with the standards shows the efficacy of the extraction procedure but it is essential to bear in mind that it may not be indicative of whether all of the tightly bound flavins were released. Rather, to facilitate the release of most of the protein bound flavins, common deflavination procedure like use of 10% TCA was done as mentioned earlier. In summary, our extraction method has higher recovery of FAD and FMN from the retina than the other previously described protocols [17, 18] and the enhanced HPLC resolution to the picomole levels will allow us to detect steady state levels of flavins in the retina and the RPE in normal and pathological conditions.

3.2. Stability of flavins during extraction

Although it is well known that the stability of FAD, FMN and RF is affected by pH and temperature [27, 34], previous methods have used extraction buffers of varying pH values ranging from pH 3.5 to 7.4. We therefore elected to evaluate the effect of different parameters on the stability of flavins including pH values at 2.8, 6.8 and 11, incubation time at 4°C (ranging from 0 to 32 hours), freezing at -20°C overnight, and freeze-thawing. These were first assessed separately with 100 pm of FAD, FMN and RF standards (Fig. 2A-C). We also assessed the effect of these parameters on FAD and FMN stability extracted from a single retina (Fig. 2D-F). Because of the low levels of RF in retinal extracts, RF was not

included in this study. Interestingly, flavin standards and retinal flavins exhibited different behaviors under these different conditions. All three standards showed maximum stability when extracted in pH 6.8 (Fig. 2A) while FAD in retinal extracts showed stability at pH values between 2.8 to 11 and with a slightly higher stability at pH 2.8. FMN, however, was most stable at pH 2.8 (Fig. 2D). The next parameter we assessed was the stability of flavins during HPLC assessments at 4°C. The HPLC auto-sampler is temperature controlled at 4°C and multiple injections can be made over time. We incubated the standards and retinal extracts for 0 to 32 hours at 4°C in the auto-sampler. We found that the standards were stable for up to 8 hours, following which the stability declined sharply (Fig. 2B). Similarly, FAD and FMN in retinal extracts were stable for up to 8 hours, after which there was a decline (Fig. 2E). We also assessed whether freeze-thawing after extraction affected the stability of both the standards and retinal flavins. One freeze-thaw cycle was sufficient to observe flavin degradation. Each subsequent cycle lead to further decline of flavins in both the standards and retinal extract (Fig. 2C&F). The results of these varied parameters established the optimal extraction and quantification conditions for flavin analysis and were adopted for the remainder of this study.

3.3. Physiological factors affecting the steady state levels of retinal flavins

3.3.1. Effect of fasting—Since RF is obtained from the diet and commercial mouse chows are fortified with RF, we tested whether the steady state levels of retinal flavins would change as a result of differential feeding. This is essential to overcome variabilities in measurements due to animal feeding status and in their physiological flavins in normal and diseased conditions. Previous reports have shown that 10 fold and 100 fold increases in dietary RF resulted in insignificant increase in retinal FAD and FMN in the rat and rabbit [17, 18]. However, it is not yet known if the feeding state can dramatically alter retinal FAD and FMN levels. We chose to fast the animals for 6 hours, an adequate amount time after feeding for the nutrients to be digested, absorbed and metabolized. In comparison to fed animals, fasted animals showed 21.5±1.08% reduction in retinal FAD ($p<0.046$) and 23.63±1.9% reduction in retinal FMN levels ($p<0.016$) (Fig. 3A&B). To avoid variabilities in assessing the steady state levels of flavin, all quantification of flavins hereafter were done 6 hour post fasting, unless otherwise mentioned.

3.3.2. Effect of light—It is well known that flavins degrade when exposed to light [39, 40]. However, this happens only when flavins are present in free (unbound) state in solution [34, 41]. For consistency, we asked the question whether dissecting the retina in light versus in complete darkness would affect retinal FAD and FMN levels. Mice were dark adapted overnight and tissues were collected from one set under complete darkness and the other set under 1200 Lux light. Quantifications of FAD and FMN are shown Fig. 3C&D. Interestingly, levels of retina FAD and FMN did not significantly change whether retinas were extracted under light or dark conditions.

3.4. Steady state levels of flavins in the retina and RPE

Having set up the optimal conditions for extraction and quantification of flavins, we next measured the steady state levels of flavins in the healthy retina. It was previously reported that the rat and rabbit retinas have high levels of FAD and FMN as compared to other tissues

[9, 18]. However, the levels of FAD and FMN in the mouse retina were not determined. Moreover, no data exists on the FAD and FMN levels present in the mammalian RPE. Comparative analysis of levels of FAD and FMN in the retina and RPE at post-natal day (P) 45 shows that the RPE harbors significantly higher levels of both FAD and FMN than the retina (Fig. 4A&B). We observe $58.8 \pm 1.04\%$ increase for FAD ($p < 0.0007$) and $881.48 \pm 10.27\%$ increase for FMN ($p < 0.0001$) in the RPE in comparison to the retina. Interestingly, we found FMN levels in the RPE are considerably higher than FAD levels. To confirm our findings by HPLC, we used a LC-MS method (Fig. 4C&D) to assess flavin levels in the mouse retina and RPE. Albeit absolute levels may be slightly different between these two methods, we found the trend was consistent- the RPE has more FAD and FMN than the retina and harbors more FMN than FAD. In order to validate that RPE flavin levels measured here were a true reflection of the flavin levels of the RPE and there was no significant contribution from the choroid and sclera (CS), we have evaluated the FAD (Fig. 4E) and FMN (Fig. 4F) levels in the PECS complex with and without the RPE. Levels in the RPE were extrapolated by subtraction of the two. As shown in Fig. 4E&F, the FAD and FMN levels in the “RPE” are still higher than the retina and the levels in the CS are low.

3.5. Effect of aging on flavin levels

Next we investigated whether retinal and RPE flavin levels change with age. Mice achieve sexual maturity at P42–56 and live up to 2.5 years in a lab setting. However, the mouse retina is fully developed by P30. As shown in Fig. 5A, retinal FAD level rises between P30 and P120 then remains at that level until P180. After p180, FAD levels steadily decline. The level is significantly lower at P360 when compared to P45, P90 and P120. FAD level in the RPE follows a similar pattern in which levels stay steady until P180, then gradually decline (Fig. 5B). Retinal FMN levels show a significant drop at P240 when compared to P90 and levels at P360 are significantly lower than the levels detected at all ages from P45 to P240 (Fig. 5C). The RPE FMN level at P240 seems to be significantly lower than both P45 and P90. It significantly drops at P360 (Fig. 5D). For both tissues, FAD and FMN levels seem stable until P180 and gradually decline afterwards demonstrating the effects of aging on levels of flavins.

To determine whether there is any correlation between the decline in flavin levels and retinal function, we evaluated full field electroretinography of mice at different ages (Fig. 6). Although structural analyses of the retinas at P30 and P360 showed no significant differences in (Fig. 6A), we observed a gradual reduction in the scotopic a-wave amplitudes as a reflection of the rod function with age (Fig. 6B&C). Scotopic a-wave at P360 is significantly lower than all ages from P30 to P120. Cone function was evaluated by photopic b-wave amplitudes and it does not seem to be affected until P90 (Fig. 6B&D). However, we detected a consistent and a significant drop by P120 followed by a decline (albeit not statistically significant) throughout the rest of the ages tested (Fig. 6D).

3.6. Effect of retinal degeneration on flavin levels

It was hypothesized that metabolism in the retina is altered during early stages of retinal degeneration [42]. It was shown that inhibiting sirtuin 6, a histone deacetylase repressor of glycolytic flux, slows down retinal degeneration resulting from reprogramming rod

photoreceptors into perpetual glycolysis and accumulation of biosynthetic intermediates. Those photoreceptors exhibited improved outer segments and vision [43]. Also, stimulation of the insulin/mTOR pathway delays cone cell death in models of retinitis pigmentosa (RP) due to mutations in rod specific genes. It has been suggested that energy starvation of cones may be the cause of cone death in RP [44]. Since flavins are directly involved in metabolism, we sought to investigate FAD and FMN levels in the retinas of *rd1*, *rd10*, *GCI^{-/-}*, and *Rho^{-/-}*, well-studied mouse models of retinal degeneration. We also evaluated two diabetic retinopathy models: *Ins2^{Akita/+}* and *db/db* mice. Both of the *rd1* and *rd10* mice arise from spontaneous recessive mutations in the β subunit of retinal phosphodiesterase (PDE) that rendered the enzyme absent in the *rd1* and partially inactive in the *rd10*. The *rd1* mouse is a fast degenerating model where rods degenerate rapidly during early postnatal development and by P30 only cones remain [45, 46]. The *rd10* mouse, on the other hand, exhibits slower rate of retinal degeneration than the *rd1* [46]. ERG responses in the *rd10* homozygous mouse are maximal at about P21, quickly declining afterwards and are absent by P60. By P25, about a third of the photoreceptors are lost [47].

Both of the *GCI^{-/-}* and *Rho^{-/-}* lines are knockouts, whereby products of the guanylate cyclase-1 gene and the rhodopsin gene were eliminated, respectively [48, 49]. Scotopic and photopic ERG amplitudes of the *GCI^{-/-}* animals are significantly affected showing nonfunctional cones and reduced rod function [48]. Cones have been observed to rapidly degenerate by P28 [50]. However, the retina of *Rho^{-/-}* develops with full complement of rod photoreceptor cells but outer segments deficient [49, 51]. At P45, the *Rho^{-/-}* retina retains 40–50% of wild-type number of rod photoreceptors [52]. Functional studies at P47 revealed cone function comparable to that of wildtype levels while rod function was not detectable [53].

We next enrolled two models with diabetic retinopathy that suffer from metabolic disorders while their retinas are either normal or degenerative at older ages. The male *Ins2^{Akita/+}* is a model for type I diabetes due to a spontaneous mutation in the insulin gene that interrupts its secretion and causes early hyperglycemia [54]. This model exhibits 27% loss of second order neurons at around P150–180 without photoreceptor loss [55, 56]. The *db/db* line, on the other hand, is a model for type II diabetes that resulted from a spontaneous mutation in a leptin receptor [57]. Although the retina in this model appears and functions normally at P42, functional deficit is observed at P112 [58] and retinal thinning from progressive loss of ganglion cells as detected by OCT is observed P196 [59].

As shown in Fig. 7A, FAD levels at P30 are significantly reduced in the retinas from *rd1*, *rd10* and *Rho^{-/-}* mice while they were equivalent to that of wild-type for *GCI^{-/-}*. FMN levels in the retinas from these three models were also reduced in comparison to wild-type (Fig. 7B). As expected, both FAD and FMN levels in the *Ins2^{Akita/+}* and the *db/db* models are significantly lower than wild-type at all ages tested. However, the reductions are more pronounced at P240 (Fig. 7C-F).

4. Discussion

In this study we utilized HPLC- and LC/MS-based techniques to determine flavin levels in mouse retina and RPE. We improved upon already existing techniques by optimizing extraction parameters and consequently increasing the sensitivity of flavin quantification in the retina. We present a micro-extraction protocol which has above 97% efficiency of recovery of FAD and FMN content from a single retina or RPE. Our enhanced sensitivity (0.1 pmol FAD, 0.1 pmol FMN and 0.01 pmol RF) compared to 2 pmol limit in previous methods [9] enables detection of lower levels of flavins, which may be critical in disease models of retinal degeneration. Furthermore, previous methods [9, 17, 18] were only able to detect flavin levels in larger mammals, i.e. rats and rabbits and required pooling of multiple retinas in order to reach the detection limit. We also evaluated and identified several experimental factors, like feeding conditions; freeze/thawing of samples, pH, elapsed time between sample preparation and measurement and/or incubation temperature that influence flavin levels. All these factors play a role in the steady state levels of flavins and may introduce unintended variability in measurements. Altogether, the results emphasize the importance of monitoring the extraction, storage and quantification methods when measuring tissue flavins.

FAD and FMN, which are produced from dietary RF, are directly involved in metabolism. Therefore, it is not surprising to report that fasting animals for six hours prior to tissue collection eliminates variabilities among the samples due to differential feedings. Previous reports have shown that the amount of RF present in diet can significantly contribute to the levels of retinal flavins [60], but previous extraction procedures were only carried out on ad libitum fed animals.

Implementing the aforementioned technique, we quantified FAD and FMN levels in the RPE for the first time. We have been able to show that despite the high metabolic activity of the retina, the RPE retains far more FAD and FMN. To re-validate this finding, we compared the retina and RPE flavin levels by an independent method by LC-MS and even though there were minor variability in the scale of difference between retinal flavins and RPE flavins, both methods indicate RPE flavins to be far higher than retinal flavins. The variability can be explained as the animals were fasted for the HPLC while those ones for LC-MS were not fasted and also, the background strain of mice used for HPLC and LC-MS were different. Moreover, to account for variability in instrument methodology, the method of extraction (methanol extraction) and detection were different for LC-MS, as mentioned in section 2.6 of Materials and Methods. All these factors contributed to the difference in between retina FAD and RPE FAD in LC-MS, but nevertheless, both methods showed higher values for both FAD and FMN in RPE, compared to the retina. The values (as shown in Fig. 4E&F) indicate that the majority of FAD and FMN in the PECS complex are indeed contributed by the RPE. It is also important to be aware, that as shown in Batey's paper [9], the level of flavins in the blood is miniscule (about 100 fold lower FAD and 50 fold lower FMN) compared to the levels in the retina. Furthermore, the amount of blood vessels in the choroid is very small and their contribution to the overall flavin levels in the PECS is considerably small. The high FAD and FMN levels in the RPE may be attributed to the fact that nutrients from the choroidal blood supply must pass the RPE to reach the retina. It has been recently

shown that RF is supplied to the retina via the blood, where RF specific transporters are present on the endothelial cells [61] while the RPE has a separate concentration dependent carrier mediated mechanism of its own [62]. Additionally, the RPE's functional activities, such as retinoid recycling and OS phagocytosis, all require high energy [63] and involve using FAD and FMN as cofactors [64].

The higher levels of flavins in both the retina and the RPE in comparison to other tissues suggest that a retaining mechanism must exist to keep flavins in the retina. Retbindin, a recently described photoreceptor specific extracellular protein that has been shown to bind RF *in vitro* [65] may provide the necessary function to retain high levels of flavins in the retina. Interestingly, elimination of retbindin led to ~50% reduction in total retinal flavins and gradual degeneration of the retina [66]. Currently, it is not well understood how the RPE is able to obtain and maintain such high levels of flavins when retbindin is not expressed [65].

We also tested the role aging plays in the steady state levels of flavins in the retina. We observed that FAD and FMN levels are significantly reduced after P180 and progressively decline thereafter. This suggests that as the retina ages, there are changes in its metabolic activity, in agreement with the earlier study showing reduced retinal metabolic activity with age [67]. This may be reflected in the gradual reduction in both rod and cone functions as animal ages, consistently observed by our group and others in the field [68, 69]. Therefore, it is imperative for future studies involving retinal flavins that the age of the animal is taken into consideration.

Measuring retinal flavins in models of retinal degeneration provided insight into flavins levels in photoreceptors versus the rest of the retina. Examining the retinas of the fast degenerating *rd1* mouse demonstrates that rod photoreceptors contribute to more than 50% of the total retinal flavins. This is based upon the fact that by ~4 weeks of age the *rd1* mice have lost all rod photoreceptors without loss of any other cell type. Interestingly, flavin levels in the *Rho*^{-/-} retina at an age where all rods are there but no OSs are present about ~50% of that in wild-type retinas. This suggests that the majority of flavins in rod photoreceptors are required for OS functions. This includes phototransduction, light-dependent protein translocation, and OS renewal and shedding. The slight reduction in flavins in the *GCI*^{-/-} retinas that lack cones reflects the small contribution of cones to the total cellular content of the mouse retina. In the *rd10* mouse model of progressive retinal degeneration, the levels are a direct reflection of the degree of rod photoreceptor cell death. Since most apoptotic cell death types and survival are energy requiring, it is not clear how reduced flavin levels influence cell choice between survival and death. However, when a cell decides to undergo cell death, it shuts down all specialized functions and dedicates the energy machinery for the death process [70]. This may require less flavins than specialized cellular functions.

There is a reduction of ~50% in both FAD and FMN levels in P240 *Ins*^{Akita/+} mice. Since these mice have been reported to have ~ 27% loss in number of second order neurons after P150 [55, 56], the 50% reduction in flavin levels must be related to another change besides the death of the second order neurons. This is supported by the more curious observation

with the *db/db* mice since they exhibit a progressive ganglion cell loss (minor contributors to total retinal cell number) there is ~50% reduction in total flavins by P240. It is safe to say that the alterations in flavin levels do not only reflect the loss in cell number but can be used to assess the overall health of the cell. The reduced FAD and FMN levels may reflect the decline in requirement for energy production through the mitochondria in favor of glycolysis under hyperglycemic conditions.

Since the mutant mice studied are all resulting from specific mutations, it is difficult to assign a causal role for flavins. However, flavin's role, though may be secondary, is likely compounding.

Lower levels of FAD have been known to increase reactive oxygen species in the cell by lowering the efficiency of the electron transport chain [71]. Recently, it was shown that reduced availability of FAD and FMN pushes the cell towards apoptosis and stress while downregulating multiple metabolic pathways [72]. There might be other factors affecting the energy metabolism in diabetes and aging conditions, but altered flavin homeostasis might be the one common precursor affecting the photoreceptors of the retina, resulting in lower rate of ATP production and higher levels of reactive oxygen species [21, 73–75].

It has been reported that patients who suffer from the Brown-Vialetto-Van Laere syndrome (BVVLS), a rare neurodegenerative disorder, have severe RF deficiency [76]. These patients suffer from severe hearing loss, cranial nerve atrophy, bulbar palsy and respiratory compromise [77, 78]. However, the effect of RF deficiency on vision in these patients has not yet been assessed in great depth. From the limited number of investigations in patient case reports, it has been shown that severe optic nerve atrophy, loss of visual acuity and nystagmus are common symptoms [79, 80]. However, these have been mostly reported in patients with mutations in *SLC52A2* and *SLC52A3* genes (two of the three known genes responsible for BVVLS) and some but not all of the patients had improved vision with RF supplementation [78]. These reports agree with earlier ones describing ocular manifestations in patients suffering from RF deficiency, where the majority experienced impaired visual acuity, poor low-light vision and mild to severe photosensitivity, even though no abnormalities were seen by fundus investigations [81].

In conclusion, this study provides an optimized methodology for improving the sensitivity of flavin detection and provides evidence to support the importance of understanding the role of flavins in aging as well as in pathological conditions.

Acknowledgments

Grants: This work was supported by the National Eye Institute (EY026499). The funder had no role in study design, data collection and analysis, decision to publish, or preparation of the manuscript. The content is solely the responsibility of the authors and does not necessarily represent the official views of NIH or any of its institutes.

References

- [1]. Barile M, Giancaspero TA, Brizio C, Panebianco C, Indiveri C, Galluccio M, et al. Biosynthesis of flavin cofactors in man: implications in health and disease. *Curr Pharm Des.* 2013;19:2649–75. [PubMed: 23116402]

- [2]. Muller F Flavin radicals: chemistry and biochemistry. *Free Radic Biol Med.* 1987;3:215–30. [PubMed: 3311900]
- [3]. Subramanian VS, Ghosal A, Kapadia R, Nabokina SM, Said HM. Molecular Mechanisms Mediating the Adaptive Regulation of Intestinal Riboflavin Uptake Process. *Plos One.* 2015;10:e0131698. [PubMed: 26121134]
- [4]. McCormick DB. The fate of riboflavin in the mammal. *Nutr Rev.* 1972;30:75–9. [PubMed: 4554035]
- [5]. Yang CS, McCormick DB. Degradation and excretion of riboflavin in the rat. *J Nutr.* 1967;93:445–53. [PubMed: 6082656]
- [6]. Powers HJ, Corfe BM, Nakano E. Riboflavin in development and cell fate. *Subcell Biochem.* 2012;56:229–45. [PubMed: 22116702]
- [7]. Gregersen N, Rhead W, Christensen E. Riboflavin responsive glutaric aciduria type II. *Prog Clin Biol Res.* 1990;321:477–94. [PubMed: 2183240]
- [8]. Powers HJ. Riboflavin (vitamin B-2) and health. *Am J Clin Nutr.* 2003;77:1352–60. [PubMed: 12791609]
- [9]. Batey DW, Eckhart CD. Identification of FAD, FMN, and riboflavin in the retina by microextraction and high-performance liquid chromatography. *Anal Biochem.* 1990;188:164–7. [PubMed: 2221357]
- [10]. Winkler BS. Glycolytic and oxidative metabolism in relation to retinal function. *J Gen Physiol.* 1981;77:667–92. [PubMed: 6267165]
- [11]. Futterman S, Kinoshita JH. Metabolism of the retina. I. Respiration of cattle retina. *J Biol Chem.* 1959;234:723–6. [PubMed: 13654250]
- [12]. Ames A, Li YY, Heher EC, Kimble CR. Energy-Metabolism of Rabbit Retina as Related to Function - High Cost of Na⁺ Transport. *Journal of Neuroscience.* 1992;12:840–53. [PubMed: 1312136]
- [13]. Ames A CNS energy metabolism as related to function. *Brain Research Reviews.* 2000;34:42–68. [PubMed: 11086186]
- [14]. Vergani L, Barile M, Angelini C, Burlina AB, Nijtmans L, Freda MP, et al. Riboflavin therapy. Biochemical heterogeneity in two adult lipid storage myopathies. *Brain.* 1999;122 (Pt 12):2401–11. [PubMed: 10581232]
- [15]. Udhayabanu T, Manole A, Rajeshwari M, Varalakshmi P, Houlden H, Ashokkumar B. Riboflavin Responsive Mitochondrial Dysfunction in Neurodegenerative Diseases. *J Clin Med.* 2017;6.
- [16]. Kennedy DO. B Vitamins and the Brain: Mechanisms, Dose and Efficacy--A Review. *Nutrients.* 2016;8:68. [PubMed: 26828517]
- [17]. Batey DW, Daneshgar KK, Eckhart CD. Flavin levels in the rat retina. *Exp Eye Res.* 1992;54:605–9. [PubMed: 1623945]
- [18]. Batey DW, Eckhart CD. Analysis of flavins in ocular tissues of the rabbit. *Invest Ophthalmol Vis Sci.* 1991;32:1981–5. [PubMed: 2055692]
- [19]. Zahn JM, Poosala S, Owen AB, Ingram DK, Lustig A, Carter A, et al. AGEMAP: a gene expression database for aging in mice. *PLoS Genet.* 2007;3:e201. [PubMed: 18081424]
- [20]. Preston CC, Oberlin AS, Holmuhamedov EL, Gupta A, Sagar S, Syed RH, et al. Aging-induced alterations in gene transcripts and functional activity of mitochondrial oxidative phosphorylation complexes in the heart. *Mech Ageing Dev.* 2008;129:304–12. [PubMed: 18400259]
- [21]. Navarro A, Boveris A. The mitochondrial energy transduction system and the aging process. *Am J Physiol Cell Physiol.* 2007;292:C670–86. [PubMed: 17020935]
- [22]. Du Y, Veenstra A, Palczewski K, Kern TS. Photoreceptor cells are major contributors to diabetes-induced oxidative stress and local inflammation in the retina. *Proc Natl Acad Sci U S A.* 2013;110:16586–91. [PubMed: 24067647]
- [23]. Sivaprasad S, Arden G. Spare the rods and spoil the retina: revisited. *Eye (Lond).* 2016;30:189–92. [PubMed: 26656085]
- [24]. Chen X, Kezic J, Bernard C, McMenamin PG. Rd8 mutation in the *Crb1* gene of CD11c-eYFP transgenic reporter mice results in abnormal numbers of CD11c-positive cells in the retina. *J Neuropathol Exp Neurol.* 2013;72:782–90. [PubMed: 23860032]

- [25]. Danciger M, Matthes MT, Yasamura D, Akhmedov NB, Rickabaugh T, Gentleman S, et al. A QTL on distal Chromosome 3 that influences the severity of light-induced damage to mouse photoreceptors. *Mammalian Genome*. 2000;11:422–7. [PubMed: 10818205]
- [26]. Kim SR, Fishkin N, Kong J, Nakanishi K, Allikmets R, Sparrow JR. Rpe65 Leu450Met variant is associated with reduced levels of the retinal pigment epithelium lipofuscin fluorophores A2E and iso-A2E. *Proceedings of the National Academy of Sciences of the United States of America*. 2004;101:11668–72. [PubMed: 15277666]
- [27]. Bessey OA, Lowry OH, Love RH. The fluorometric measurement of the nucleotides of riboflavin and their concentration in tissues. *J Biol Chem*. 1949;180:755–69. [PubMed: 18135810]
- [28]. Ly A, Merl-Pham J, Priller M, Gruhn F, Senninger N, Ueffing M, et al. Proteomic Profiling Suggests Central Role Of STAT Signaling during Retinal Degeneration in the rd10 Mouse Model. *J Proteome Res*. 2016;15:1350–9. [PubMed: 26939627]
- [29]. Cavusoglu N, Thierse D, Mohand-Said S, Chalmel F, Poch O, Van-Dorsselaer A, et al. Differential proteomic analysis of the mouse retina: the induction of crystallin proteins by retinal degeneration in the rd1 mouse. *Mol Cell Proteomics*. 2003;2:494–505. [PubMed: 12832458]
- [30]. Kanan Y, Centola M, Bart F, Al-Ubaidi MR. Analysis of genes differentially expressed during retinal degeneration in three mouse models. *Adv Exp Med Biol*. 2010;664:3–13. [PubMed: 20237996]
- [31]. Du J, Linton JD, Hurley JB. Probing Metabolism in the Intact Retina Using Stable Isotope Tracers. *Methods Enzymol*. 2015;561:149–70. [PubMed: 26358904]
- [32]. Cheng T, Peachey NS, Li S, Goto Y, Cao Y, Naash MI. The effect of peripherin/rds haploinsufficiency on rod and cone photoreceptors. *J Neurosci*. 1997;17:8118–28. [PubMed: 9334387]
- [33]. Akimoto M, Sato Y, Okubo T, Todo H, Hasegawa T, Sugibayashi K. Conversion of FAD to FMN and riboflavin in plasma: effects of measuring method. *Biol Pharm Bull*. 2006;29:1779–82. [PubMed: 16880644]
- [34]. Sheraz MA, Kazi SH, Ahmed S, Anwar Z, Ahmad I. Photo, thermal and chemical degradation of riboflavin. *Beilstein J Org Chem*. 2014;10:1999–2012. [PubMed: 25246959]
- [35]. Hefti MH, Vervoort J, van Berkel WJ. Dechlorination and reconstitution of flavoproteins. *European journal of biochemistry*. 2003;270:4227–42. [PubMed: 1462288]
- [36]. Mayhew SG. Studies on flavin binding in flavodoxins. *Biochimica et biophysica acta*. 1971;235:289–302. [PubMed: 5317635]
- [37]. Haines DC, Sevrioukova IF, Peterson JA. The FMN-binding domain of cytochrome P450BM3: resolution, reconstitution, and flavin analogue substitution. *Biochemistry*. 2000;39:9419–29. [PubMed: 10924137]
- [38]. Vinas P, Balsalobre N, Lopez-Erroz C, Hernandez-Cordoba M. Liquid chromatographic analysis of riboflavin vitamers in foods using fluorescence detection. *J Agric Food Chem*. 2004;52:1789–94. [PubMed: 15053510]
- [39]. Bishop AM, Fernandez C, Whitehead RD Jr., Morales AP, Barr DB, Wilder LC, et al. Quantification of riboflavin in human urine using high performance liquid chromatography-tandem mass spectrometry. *J Chromatogr B Analyt Technol Biomed Life Sci*. 2011;879:1823–6.
- [40]. Treadwell GE, Cairns WL, Metzler DE. Photochemical degradation of flavins. V. Chromatographic studies of the products of photolysis of riboflavin. *J Chromatogr*. 1968;35:376–88. [PubMed: 5658569]
- [41]. Choe E, Huang RM, Min DB. Chemical reactions and stability of riboflavin in foods. *Journal of Food Science*. 2005;70:R28–R36.
- [42]. Griciuc A, Roux MJ, Merl J, Giangrande A, Hauck SM, Aron L, et al. Proteomic survey reveals altered energetic patterns and metabolic failure prior to retinal degeneration. *J Neurosci*. 2014;34:2797–812. [PubMed: 24553922]
- [43]. Zhang L, Du J, Justus S, Hsu CW, Bonet-Ponce L, Wu WH, et al. Reprogramming metabolism by targeting sirtuin 6 attenuates retinal degeneration. *J Clin Invest*. 2016;126:4659–73. [PubMed: 27841758]
- [44]. Punzo C, Kornacker K, Cepko CL. Stimulation of the insulin/mTOR pathway delays cone death in a mouse model of retinitis pigmentosa. *Nat Neurosci*. 2009;12:44–52. [PubMed: 19060896]

- [45]. Pennesi ME, Michaels KV, Magee SS, Maricle A, Davin SP, Garg AK, et al. Long-Term Characterization of Retinal Degeneration in rd1 and rd10 Mice Using Spectral Domain Optical Coherence Tomography. *Investigative Ophthalmology & Visual Science*. 2012;53:4644–56. [PubMed: 22562504]
- [46]. Chang B, Hawes NL, Hurd RE, Davisson MT, Nusinowitz S, Heckenlively JR. Retinal degeneration mutants in the mouse. *Vision Res*. 2002;42:517–25. [PubMed: 11853768]
- [47]. Gargini C, Terzibasi E, Mazzoni F, Strettoi E. Retinal organization in the retinal degeneration 10 (rd10) mutant mouse: A morphological and ERG study. *Journal of Comparative Neurology*. 2007;500:222–38. [PubMed: 17111372]
- [48]. Yang RB, Robinson SW, Xiong WH, Yau KW, Birch DG, Garbers DL. Disruption of a retinal guanylyl cyclase gene leads to cone-specific dystrophy and paradoxical rod behavior. *Journal of Neuroscience*. 1999;19:5889–97. [PubMed: 10407028]
- [49]. Humphries MM, Rancourt D, Farrar GJ, Kenna P, Hazel M, Bush RA, et al. Retinopathy induced in mice by targeted disruption of the rhodopsin gene. *Nature Genetics*. 1997;15:216–9. [PubMed: 9020854]
- [50]. Boye SE, Boye SL, Pang JJ, Ryals R, Everhart D, Umino Y, et al. Functional and Behavioral Restoration of Vision by Gene Therapy in the Guanylate Cyclase-1 (GC1) Knockout Mouse. *Plos One*. 2010;5:e11306. [PubMed: 20593011]
- [51]. Lem J, Krasnoperova NV, Calvert PD, Kosaras B, Cameron DA, Nicolo M, et al. Morphological, physiological, and biochemical changes in rhodopsin knockout mice. *Proc Natl Acad Sci U S A*. 1999;96:736–41. [PubMed: 9892703]
- [52]. Jaissle GB, May CA, Reinhard J, Kohler K, Fauser S, Lutjen-Drecoll E, et al. Evaluation of the rhodopsin knockout mouse as a model of pure cone function. *Investigative Ophthalmology & Visual Science*. 2001;42:506–13. [PubMed: 11157890]
- [53]. Toda K, Bush RA, Humphries P, Sieving PA. The electroretinogram of the rhodopsin knockout mouse. *Visual Neuroscience*. 1999;16:391–8. [PubMed: 10367972]
- [54]. Mathews CE, Langley SH, Leiter EH. New mouse model to study islet transplantation in insulin-dependent diabetes mellitus. *Transplantation*. 2002;73:1333–6. [PubMed: 11981430]
- [55]. Barber AJ, Antonetti DA, Kern TS, Reiter CEN, Soans RS, Krady JK, et al. The Ins2(Akita) mouse as a model of early retinal complications in diabetes. *Investigative Ophthalmology & Visual Science*. 2005;46:2210–8. [PubMed: 15914643]
- [56]. Han Z, Guo J, Conley SM, Naash MI. Retinal angiogenesis in the Ins2(Akita) mouse model of diabetic retinopathy. *Invest Ophthalmol Vis Sci*. 2013;54:574–84. [PubMed: 23221078]
- [57]. Tartaglia LA, Dembski M, Weng X, Deng N, Culpepper J, Devos R, et al. Identification and expression cloning of a leptin receptor, OB-R. *Cell*. 1995;83:1263–71. [PubMed: 8548812]
- [58]. Bogdanov P, Corraliza L, Villena JA, Carvalho AR, Garcia-Arumi J, Ramos D, et al. The db/db mouse: a useful model for the study of diabetic retinal neurodegeneration. *PLoS One*. 2014;9:e97302. [PubMed: 24837086]
- [59]. Yang Q, Xu YD, Xie P, Cheng HX, Song QL, Su T, et al. Retinal Neurodegeneration in db/db Mice at the Early Period of Diabetes. *Journal of Ophthalmology*. 2015;2015:9.
- [60]. Eckhert CD, Hsu MH, Batey DW. Effect of dietary riboflavin on retinal density and flavin concentrations in normal and dystrophic RCS rats. *Prog Clin Biol Res*. 1989;314:331–41. [PubMed: 2608666]
- [61]. Kubo Y, Yahata S, Miki S, Akanuma SI, Hosoya KI. Blood-to-retina transport of riboflavin via RFVTs at the inner blood-retinal barrier. *Drug Metab Pharmacokinet*. 2017;32:92–9. [PubMed: 27964953]
- [62]. Said HM, Wang S, Ma TY. Mechanism of riboflavin uptake by cultured human retinal pigment epithelial ARPE-19 cells: possible regulation by an intracellular Ca²⁺-calmodulin-mediated pathway. *J Physiol*. 2005;566:369–77. [PubMed: 15878949]
- [63]. Wong-Riley MT. Energy metabolism of the visual system. *Eye Brain*. 2010;2:99–116. [PubMed: 23226947]
- [64]. Parker RO, Crouch RK. Retinol dehydrogenases (RDHs) in the visual cycle. *Experimental Eye Research*. 2010;91:788–92. [PubMed: 20801113]

- [65]. Kelley RA, Al-Ubaidi MR, Naash MI. Retbindin is an extracellular riboflavin-binding protein found at the photoreceptor/retinal pigment epithelium interface. *J Biol Chem.* 2015;290:5041–52. [PubMed: 25542898]
- [66]. Kelley RA, Al-Ubaidi MR, Sinha T, Genc AM, Makia MS, Ikelle L, et al. Ablation of the riboflavin-binding protein retbindin reduces flavin levels and leads to progressive and dosedependent degeneration of rods and cones. *J Biol Chem.* 2017;292:21023–34. [PubMed: 29079576]
- [67]. Harman D The aging process. *Proc Natl Acad Sci U S A.* 1981;78:7124–8. [PubMed: 6947277]
- [68]. Gresh J, Goletz PW, Crouch RK, Rohrer B. Structure-function analysis of rods and cones in juvenile, adult, and aged C57bl/6 and Balb/c mice. *Vis Neurosci.* 2003;20:211–20. [PubMed: 12916741]
- [69]. Li C, Cheng M, Yang H, Peachey NS, Naash MI. Age-related changes in the mouse outer retina. *Optom Vis Sci.* 2001;78:425–30. [PubMed: 11444632]
- [70]. Kanan Y, Matsumoto H, Song H, Sokolov M, Anderson RE, Rajala RV. Serine/threonine kinase akt activation regulates the activity of retinal serine/threonine phosphatases, PHLPP and PHLPP1. *J Neurochem.* 2010;113:477–88. [PubMed: 20089132]
- [71]. Cornelius N, Byron C, Hargreaves I, Guerra PF, Furdek AK, Land J, et al. Secondary coenzyme Q10 deficiency and oxidative stress in cultured fibroblasts from patients with riboflavin responsive multiple Acyl-CoA dehydrogenation deficiency. *Hum Mol Genet.* 2013;22:3819–27. [PubMed: 23727839]
- [72]. Xin ZH, Pu LL, Gao WN, Wang YW, Wei JY, Shi TL, et al. Riboflavin deficiency induces a significant change in proteomic profiles in HepG2 cells. *Scientific Reports.* 2017;7. [PubMed: 28127057]
- [73]. Parapuram SK, Cojocaru RI, Chang JR, Khanna R, Brooks M, Othman M, et al. Distinct Signature of Altered Homeostasis in Aging Rod Photoreceptors: Implications for Retinal Diseases. *Plos One.* 2010;5.
- [74]. Calderon GD, Juarez OH, Hernandez GE, Punzo SM, De la Cruz ZD. Oxidative stress and diabetic retinopathy: development and treatment. *Eye (Lond).* 2017;31:1122–30. [PubMed: 28452994]
- [75]. Czajka A, Malik AN. Hyperglycemia induced damage to mitochondrial respiration in renal mesangial and tubular cells: Implications for diabetic nephropathy. *Redox Biol.* 2016;10:100–7. [PubMed: 27710853]
- [76]. Johnson JO, Gibbs JR, Megarbane A, Urtizberea JA, Hernandez DG, Foley AR, et al. Exome sequencing reveals riboflavin transporter mutations as a cause of motor neuron disease. *Brain.* 2012;135:2875–82. [PubMed: 22740598]
- [77]. Malafrente P, Clark HB, Castaneda-Sanchez I, Raisanen J, Hatanpaa KJ. Brown-Vialetto-Van Laere syndrome: clinical and neuropathologic findings with immunohistochemistry for C20orf54 in three affected patients. *Pediatr Dev Pathol.* 2013;16:364–71. [PubMed: 23688382]
- [78]. Bosch AM, Stroek K, Abeling NG, Waterham HR, Ijlst L, Wanders RJ. The Brown-Vialetto-Van Laere and Fazio Londe syndrome revisited: natural history, genetics, treatment and future perspectives. *Orphanet J Rare Dis.* 2012;7:83. [PubMed: 23107375]
- [79]. Wilmshurst JM, Ouvrier RA. Chapter 22 - Neuropathies Secondary to Systemic Disorders A2 - Darras, Basil T In: Jones HR, Ryan MM, Vivo DCD, editors. *Neuromuscular Disorders of Infancy, Childhood, and Adolescence (Second Edition)*. San Diego: Academic Press; 2015 p. 41830.
- [80]. Haack TB, Makowski C, Yao Y, Graf E, Hempel M, Wieland T, et al. Impaired riboflavin transport due to missense mutations in SLC52A2 causes Brown-Vialetto-Van Laere syndrome. *J Inherit Metab Dis.* 2012;35:943–8. [PubMed: 22864630]
- [81]. Kruse HD, Sydenstricker VP, Sebrell WH, Cleckley HM. *Ocular manifestations of ariboflavinosis*. Washington,: U.S Govt. print. off.; 1940.

Highlights

- Optimized method with enhanced sensitivity for flavin quantification
- Flavin levels found to be far higher in RPE than the retina
- Decline in flavin homeostasis precedes decline in retinal function with age for both retina and RPE
- Retinal degeneration and diabetic retinopathy have reduced flavins indicating altered metabolism

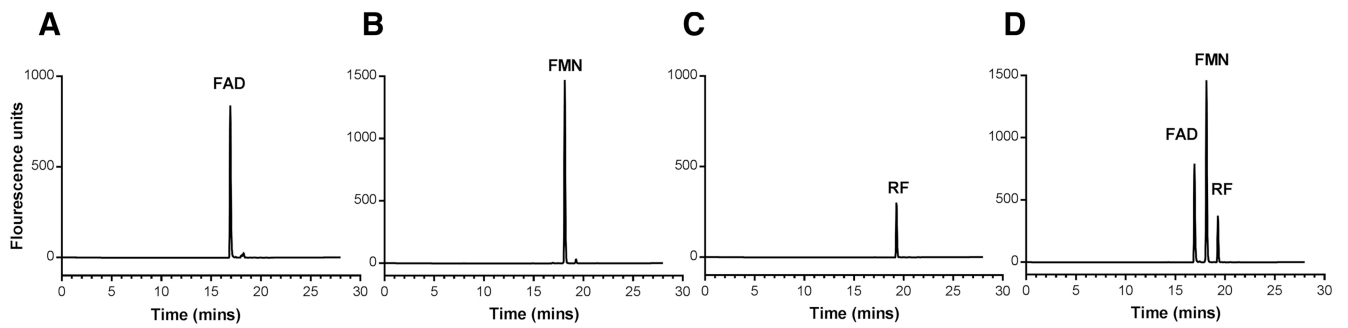


Figure 1.

HPLC profile of FAD, FMN and RF. (A) HPLC profile of 60 pmole of FAD standard showing 16.9 min of retention time. (B) HPLC profile of 60 pmole of FMN standard showing 18.1 min of retention time. (C) HPLC profile of 450 nmole of RF showing retention time of 19.2 min. (D) HPLC profile of the three flavin standards at the amounts used in A-C are showing their retention times and separation of their peaks.

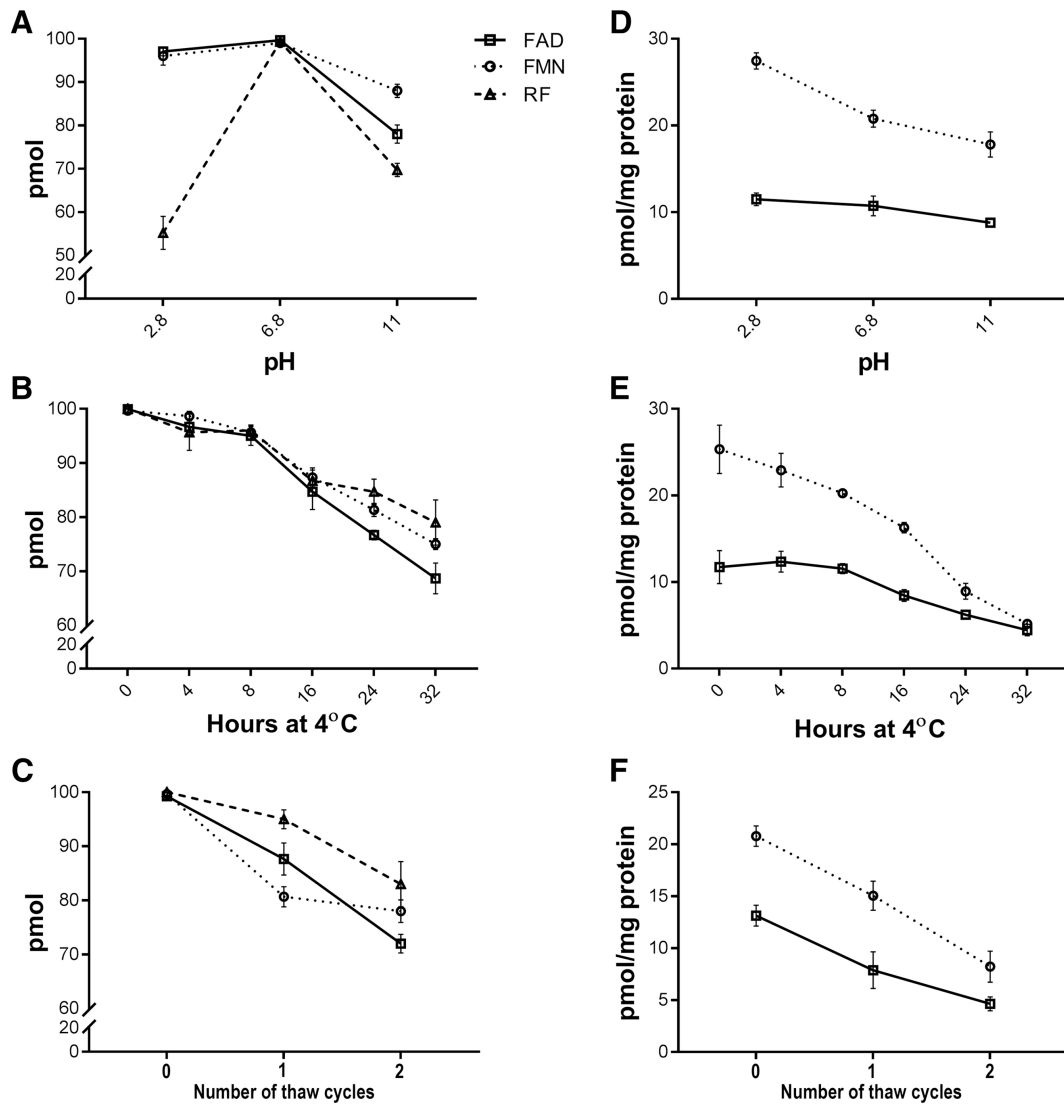


Figure 2.

Stability of FAD, FMN and RF at different conditions. (A) Stability of 100 pmol of each flavin standard at different pH at 4°C. (B) Effect of incubation at 4°C on stability of 100 pmol of each flavin standard at pH 6.8. (C) Effects of freeze-thawing on stability of 100 pmol of each standard at pH 6.8. (D) Effect of pH on the stability of retinal flavins at 4°C. (E) Effect of incubation time at 4°C on the stability of retinal flavins at pH 6.8. (F) Effect of freeze-thawing on the stability of retinal flavins at pH 6.8. (n=6 for each measurement).

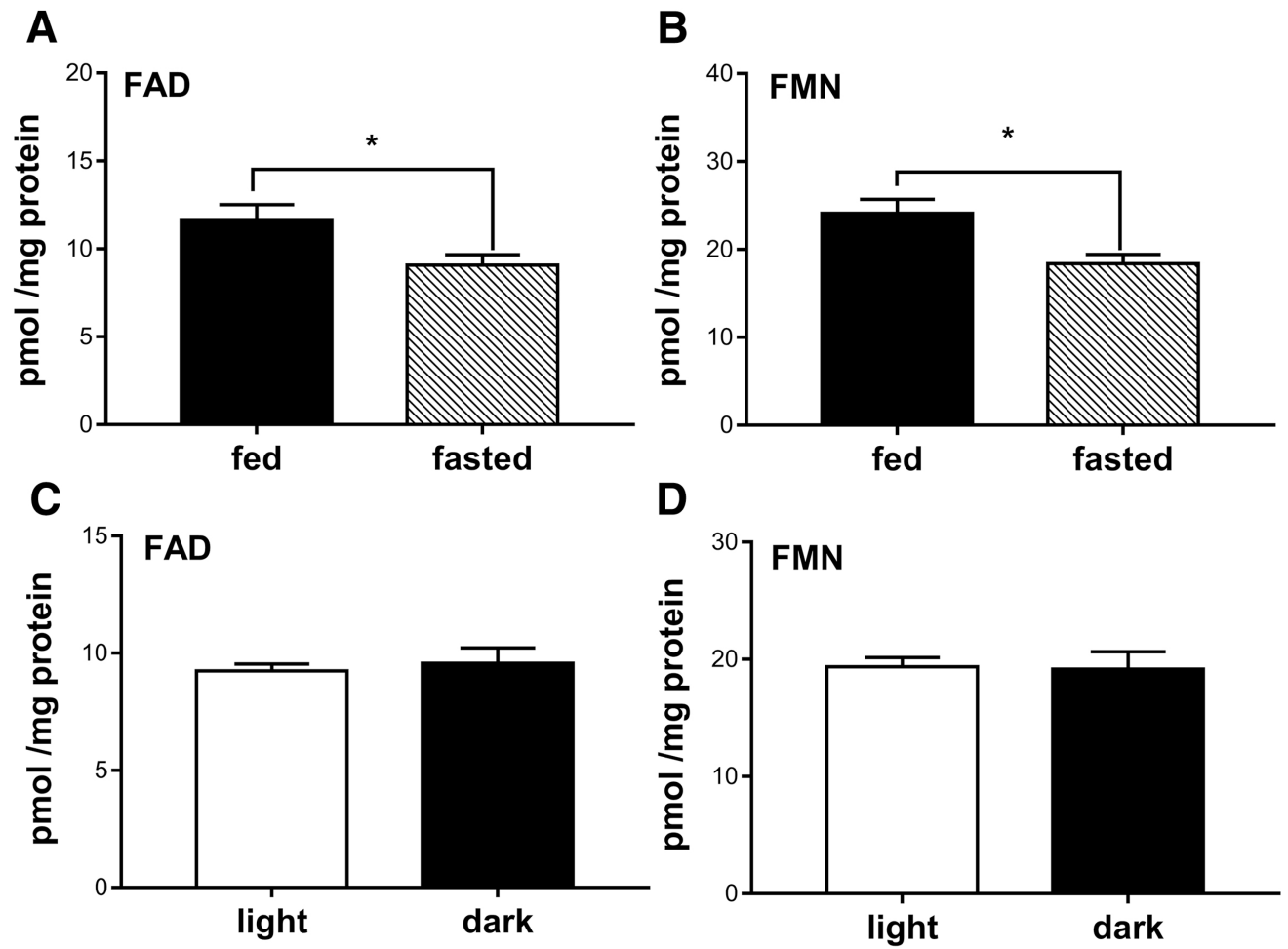


Figure 3. Steady state levels of retinal flavins. (A&B) Levels of FAD and FMN in retinas of 6 hours fasted and ad libitum fed mice (* for FAD $p < 0.046$ and * for FMN $p < 0.016$). (C&D) Levels of FAD and FMN from retinas of mice collected in dark or in light, respectively. Unpaired t-test was used to assess significance. Values were represented as pmol normalized to mg retinal proteins.

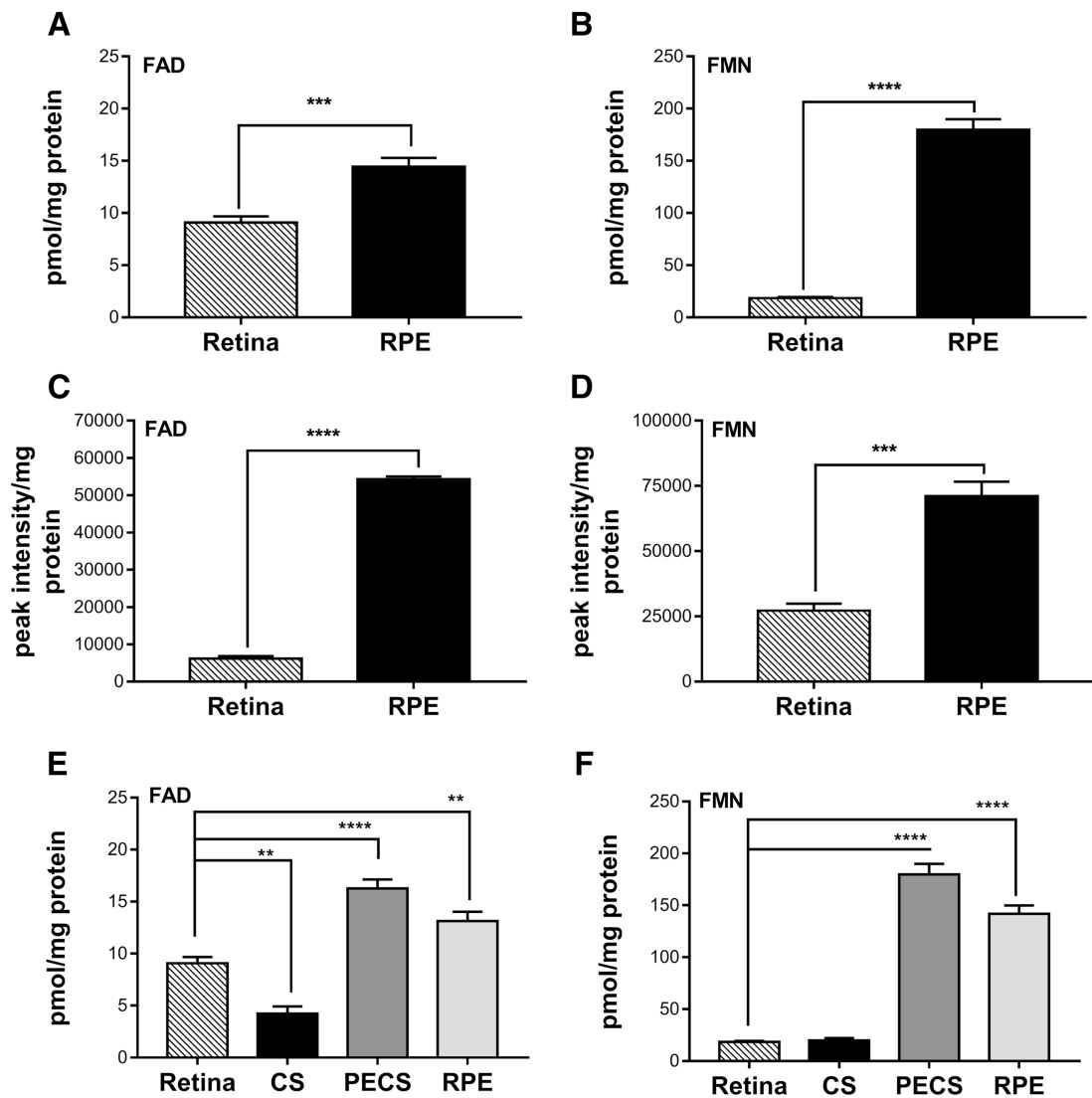


Figure 4.

Basal physiological levels of flavins in the mouse retina and RPE. (A&B) FAD and FMN levels from retinas and RPE of P45 mice assessed by HPLC (** for FAD $p < 0.0007$ and **** for FMN $p < 0.0001$). (C&D) FAD and FMN from retinas and RPE of P42 mice quantified by LC-MS (**** for FAD $p < 0.0001$ and *** for FMN $p < 0.0004$). (E&F) FAD and FMN levels from retinas, choroid and sclera complex (CS), PECS complex and RPE by HPLC. Unpaired t-test was used to assess significance for A-D and one way ANOVA for E&F. Values obtained from HPLC are presented as pmol/mg protein and those obtained from LC-MS are expressed as peak intensity per mg protein ($n=12$ for each of the retina and RPE measured by HPLC, $n=4$ for each of the retina and RPE measured by LC-MS and $n=4$ for each of retina, CS and PECS measured by HPLC).

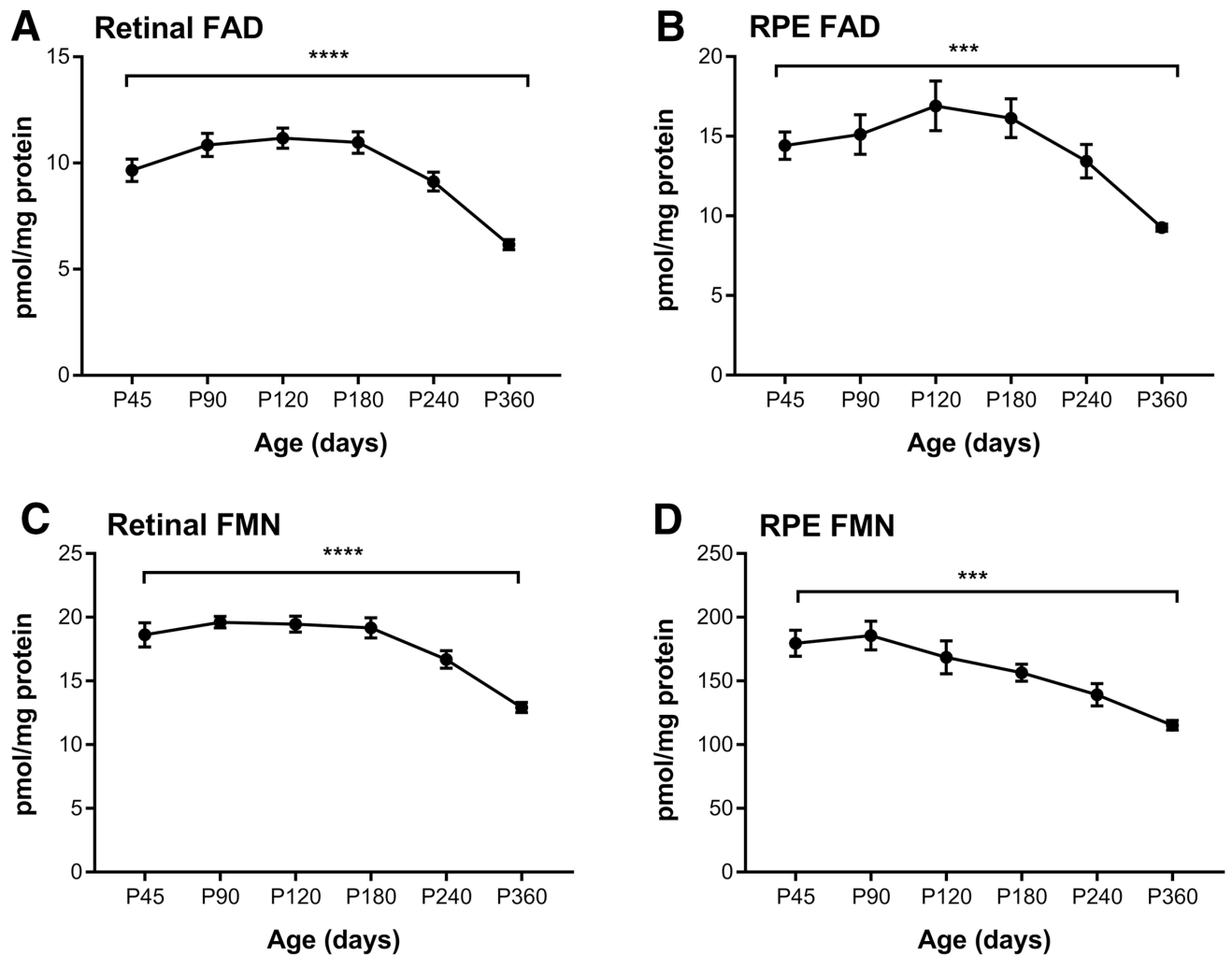


Figure 5. Age-related changes on the steady state levels of flavins in the mouse retina and RPE. (A&C) FAD and FMN levels in retina of mice at the indicated ages, respectively. (B&D) FAD and FMN levels in mouse RPE at the indicated ages, respectively. One way ANOVA was used to assess significance. Values are presented as pmol/mg proteins. ****= p -value <0.0001 , ***= p -value <0.001 , (n=10 for each age for the FAD and FMN measurement).

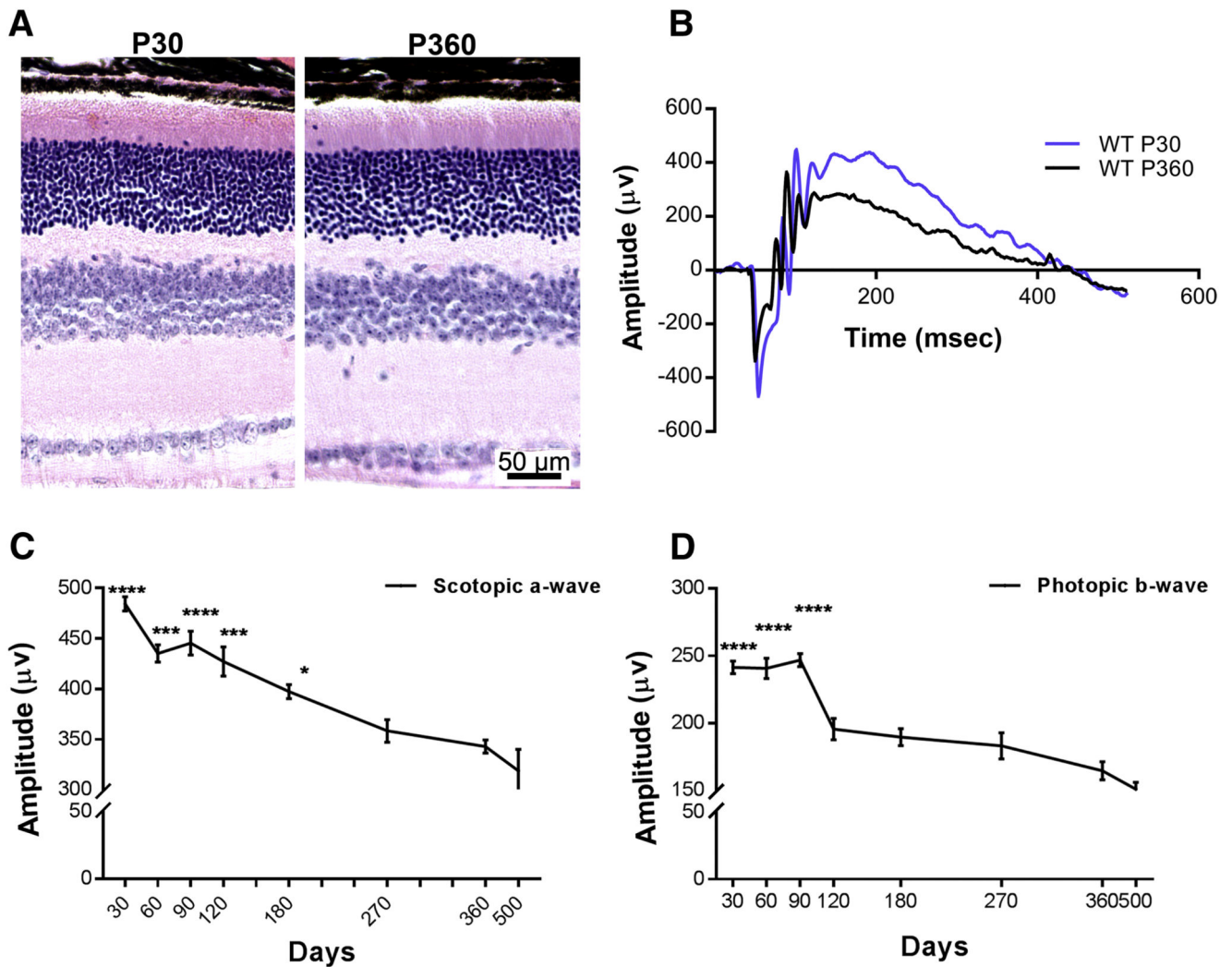
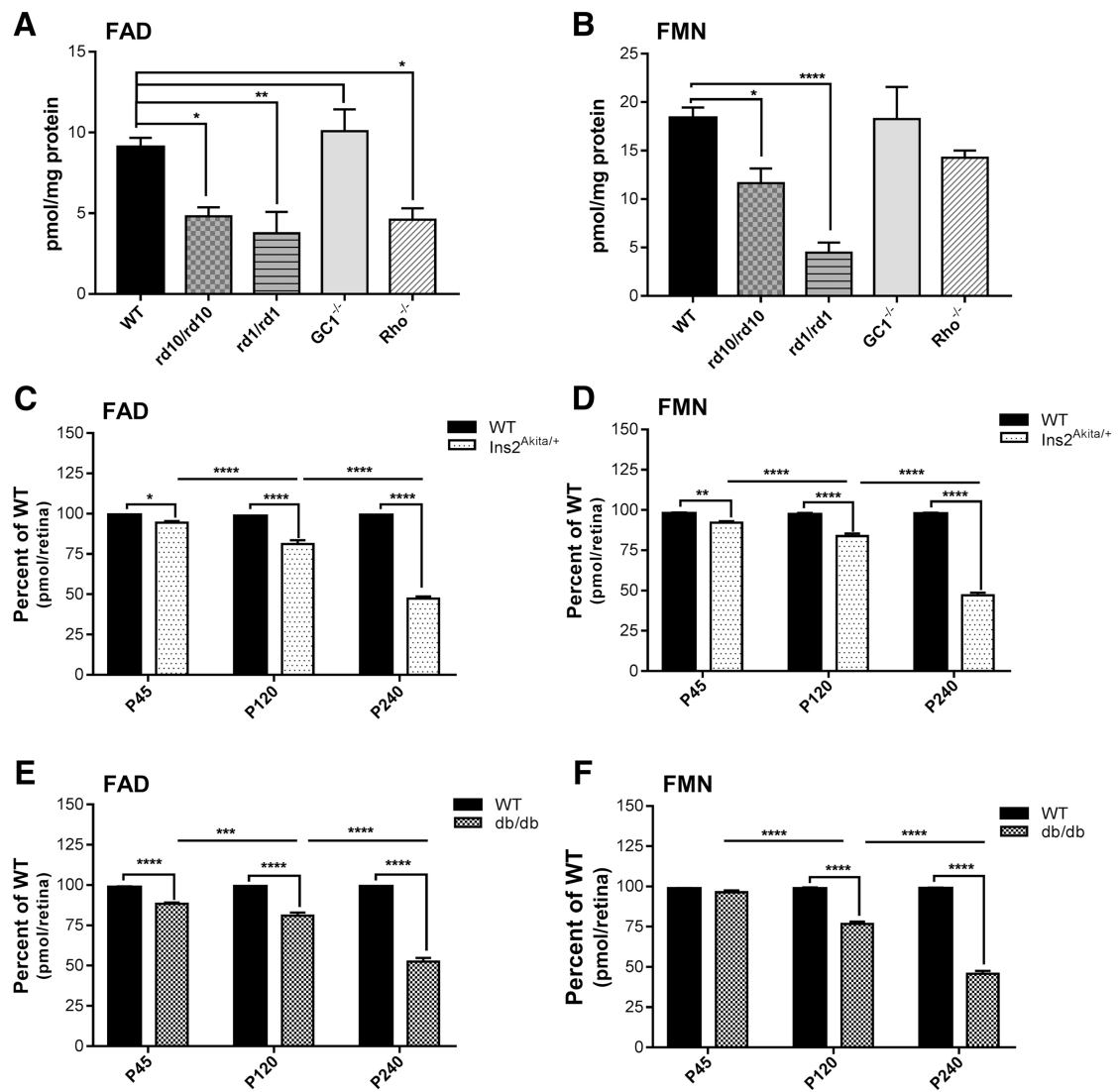


Figure 6. Effect of aging on retinal structure and function. (A) Retinal histology at P30 and P360. (B) Representative scotopic electroretinographic wave forms recorded from wild-type mice at P30 (blue) and P360 (black). (C&D) Scotopic a-wave and photopic b-wave amplitudes recorded from mice at the indicated ages, respectively. Comparisons were made with the respective values at P360 and the statistical test used was one way ANOVA with significance being presented at the top of the respective time point. ****= p -value <0.0001 , ***= p -value <0.001 , **= p -value <0.01 *= p -value <0.05 ($n=77$ for P30, $n=29$ for P60, $n=48$ for P90, $n=26$ for P120, $n=35$ for P180, $n=20$ for P270, $n=14$ for P360).

**Figure 7.**

Steady state levels of retinal flavins in models of retinal degeneration and diabetic retinopathy. (A&B) FAD and FMN levels (pmol/mg protein) in retinas from the indicated mouse models of retinal degeneration at P30, respectively. (C&D) FAD and FMN levels in retina of *Ins2^{Akita/+}* mice at the indicated ages, respectively. (E&F) FAD and FMN levels from retina of *db/db* mice at the indicated ages, respectively. Comparisons were made with the respective age matched wild-type controls and the statistical test used was One-way ANOVA with Holm-Sidak's multiple comparisons test. Values (pmol/retina) are presented as percent of wild-type. ****=*p*-value<0.0001, ***=*p*-value<0.001, **=*p*-value<0.01, *=*p*-value<0.05 (n=6 for WT, n=5 for each of *rd10*, *rd1* and *Rho^{-/-}*, n=4 for *GCI^{-/-}*, n=10 for each age group of *Ins2^{Akita/+}* and *db/db*).

Table 1

Optimized gradient method for HPLC separation of flavins

Time (min)	% Solution A*	% Solution B*
0	95	5
6.25	95	5
18.75	75	25
19	50	50
22.25	50	50
22.5	95	5
28.5	95	5

Solution A, 1X phosphate buffer (50mM) pH=3.1, solution B is acetonitrile; flow rate is 0.8ml/minute.

Author Manuscript

Author Manuscript

Author Manuscript

Author Manuscript

Table 2

Linearity of the HPLC gradient method

	Range	Equation	Correlation coefficient
FAD	0.1 pmol-50 nmol	$y = 1345x - 521.84$	0.992
FMN	0.1 pmol-10 nmol	$y = 155.95x - 9.7702$	0.997
Rf	0.01 pmol-10 nmol	$y = 6458x - 19.626$	0.995

Author Manuscript

Author Manuscript

Author Manuscript

Author Manuscript

Table 3

Recovery and reproducibility

	Spiked concentration (pmol)	Recovery (%)	
		Retina	RPE
FAD	100	98.6±1.3	97.3±4.6
FMN	100	99.2±2.7	97.1±3.3
Rf	100	96.2±6.1	95.1±1.1

Author Manuscript

Author Manuscript

Author Manuscript

Author Manuscript